

# Kondo effect near the Van Hove singularity in biased bilayer graphene

Stanisław Lipiński\* and Damian Krychowski

*Institute of Molecular Physics, Polish Academy of Sciences*

*M. Smoluchowskiego 17, 60-179 Poznań, Poland*

## Abstract

Magnetic impurity adsorbed on one of the carbon planes of a bilayer graphene is studied. The formation of the many-body  $SU(2)$  and  $SU(4)$  resonances close to the bandgap is analyzed within the mean field Kotliar-Ruckenstein slave boson approach. Impact of enhanced hybridization and magnetic instability of bilayer doped near the Van Hove singularity on the screening of magnetic moment is discussed.

PACS numbers: 73.20.Hb, 73.22.Pr, 75.20.Hr

Keywords: electronic structure, graphene bilayer, Kondo effect, valence fluctuations

---

\*Electronic address: lipinski@ifmpan.poznan.pl; Fax: +48-61-868-45-24

## I. INTRODUCTION

Bilayer graphene (BLG) is a quasi-two-dimensional gapless chiral electron-hole system with parabolic bands with conduction and valence branches touching at a point [1]. The AB Bernal stacked bilayer has inversion symmetry. The non-zero bandgap can be induced by breaking this symmetry e.g. by applying transverse electric field. As opposed to conventional semiconductors, bandgap of BLG can be tuned, what is the reason of technological importance of this material [2]. The density of states (DOS) of biased BLG has the square-root singularities at the band edges, just like in one-dimensional systems. It is well known that electronic instabilities are expected at the crossing of the Fermi level ( $E_F$ ) with Van Hove singularity (VHS). The possibility of magnetic ordering in bilayer graphene has been discussed in several papers [3–5]. Since the chemical potential of BLG can be tuned one expects that formation of local magnetic moment can be also controlled by gate voltage. A strong enhancement of DOS at the Fermi level increases hybridization, what moves impurity state towards mixed valence (MV) regime or even suppresses the many body resonance. It is a challenging problem to discuss Kondo or mixed valence resonance under above mentioned conditions taking also into account possible magnetic instability in BLG matrix. Understanding of the interplay of these competitive effects is important for prospect of Van Hove singularity engineering.

## II. MODEL

Bilayer graphene [1] is composed of two coupled honeycomb lattices of carbon atoms. We consider AB-Bernal stacking, where the top layer has its A sublattice on top of sublattice B of the bottom layer. Indices 1 and 2 are used to label top and bottom layers, respectively. In the tight binding approximation the BLG Hamiltonian reads:

$$\begin{aligned} \mathcal{H}_{BLG} = & \sum_{p\alpha i\sigma} -(-1)^\alpha (V_g/2) n_{\alpha i\sigma}^{(p)} + \mathcal{U}_g \sum_{p\alpha i\sigma} n_{\alpha i\uparrow}^{(p)} n_{\alpha i\downarrow}^{(p)} - t \sum_{\langle ij \rangle \alpha} (a_{\alpha i\sigma}^+ b_{\alpha j\sigma} + h.c.) \\ & - t_\perp \sum_i (a_{1i\sigma}^+ b_{2i\sigma} + h.c.), \end{aligned} \quad (1)$$

where  $a_{\alpha i\sigma}$  ( $b_{\alpha i\sigma}$ ) annihilates electron on sublattice  $A(B)$  in plane  $\alpha = 1, 2$  at site  $i$ ,  $\langle ij \rangle$  represent a pair of in-plane nearest neighbors,  $p$  numerates sublattices,  $t$ ,  $t_\perp$  denote the in-plane and interlayer hopping integrals respectively,  $\mathcal{U}_g$  measures on-site graphene Coulomb

interaction and  $V_g$  is the electrostatic bias applied to the two planes. The value of  $t$  ( $t = 2.7$  eV) is taken as the energy unit and we assume  $t_\perp = 0.2$ ,  $\mathcal{U}_g = 1$  [5]. It is out of scope of the present paper to discuss the details of magnetic instabilities near VHS (see for e.g. [3–5]). For simplicity, following [5] we adopt the mean field approach and define ferromagnetic ground state characterized by unequal magnetizations of the layers and different electron densities:

$$\langle n_{\alpha i \sigma}^{(p)} \rangle = \frac{n - (-1)^\alpha \Delta n}{8} + \sigma \frac{m - (-1)^\alpha \Delta m}{8}, \quad (2)$$

where  $n$  and  $m$  denote electron density and magnetization per unit cell respectively and  $\Delta n$ ,  $\Delta m$  the corresponding differences between the layers. The analysis presented in this paper is addressed to TM adatoms located in the energetically favorable position -centre of a hexagon (hollow site). The symmetry of hollow site in BLG is  $C_{3v}$  and five d orbitals split into two orbital doublets corresponding to two-dimensional representation ( $E$ ) and a singlet of one-dimensional representation  $A_1$ . In Kondo physics the crucial role play electrons with unpaired spins. To get a microscopic insight into the orbital occupations of the concrete impurity ab initio calculations are required [6]. In our model analysis based on Anderson Hamiltonian the picture is simplified by considering only the pair of orbitally degenerate states ( $SU(4)$ ) or by discussing even simpler case when symmetry is further reduced to two spin-orbitals ( $SU(2)$ ) [6]. The impurity Hamiltonian for  $SU(4)$  symmetry reads:

$$\mathcal{H}_{imp}^{[m]} = \sum_{m\sigma} \epsilon_0 n_{m\sigma} + \mathcal{U}_0 \sum_m n_{m\uparrow} n_{m\downarrow} + V^{[m]} \sum_{m\sigma} (c_{m\sigma}^+ d_{m\sigma} + h.c.), \quad (3)$$

with  $|m| = 1, 2$ ,  $\epsilon_0 = -0.5$ .  $c_{m\sigma} = (1/\sqrt{6}) \sum_i (e^{im\varphi_{iA}} a_{1i\sigma} + e^{im\varphi_{iB}} b_{1i\sigma})$  and  $\varphi_{iA(B)}$  denotes the angle between a fixed crystalline axes and the bond from site  $i$  to the impurity. To discuss the many-body problem we use mean field Kotliar-Ruckenstein slave boson approach [7] in the infinite impurity Coulomb interaction limit  $\mathcal{U}_0 \rightarrow \infty$ . The finite  $\mathcal{U}_0$  limit will be discussed elsewhere. Three introduced auxiliary boson fields  $e$ ,  $p_{m\sigma}$  ( $\sigma = \pm 1$ ) project respectively onto the empty or single occupied state (with spin up or down). The slave boson Hamiltonian reads:

$$\begin{aligned} \mathcal{H}_{imp} = & \sum_{m\sigma} \epsilon_0 f_{m\sigma}^+ f_{m\sigma} + V^{[m]} \sum_{m\sigma} (c_{m\sigma}^+ z_{m\sigma} f_{m\sigma} + h.c.) \\ & + \lambda(I - 1) + \sum_{m\sigma} \lambda_{m\sigma} (Q_{m\sigma} - f_{m\sigma}^+ f_{m\sigma}) \end{aligned} \quad (4)$$

The terms with Langrange multipliers  $\lambda$  and  $\lambda_{m\sigma}$  are incorporated to prevent double occupancy and to fulfill the complete relations.  $I = e^+e + \sum_{m\sigma} p_{m\sigma}^+ p_{m\sigma}$ ,  $Q_{m\sigma} = p_{m\sigma}^+ p_{m\sigma}$ ,  $z_{m\sigma} = e^+ p_{m\sigma} / (\sqrt{Q_{m\sigma}} \sqrt{1 - Q_{m\sigma}})$  and pseudofermion operator  $f_{m\sigma} = z_{m\sigma} d_{m\sigma}$ . The slave boson parameters  $e, p_\sigma$  ( $p_\sigma = p_{m\sigma} = p_{-m\sigma}$ ),  $\lambda$  and  $\lambda_\sigma$  are determined minimizing the ground state energy of (4).

### III. RESULTS AND DISCUSSION

Fig. 1 illustrates DOS of the mean field ferromagnetic state of BLG ( $\varrho_\sigma(E)$ ) for Fermi level located close to the upper gap edge. The spin splitting of near-gap conduction band states is visible. The low energy band structure presented in the inset shows a *Mexican hat* dispersion. The wave vector  $q$  measures the deviation from the centre of the valley  $K_\pm = \pm(4\pi/3a, 0)$ , ( $k = K_\pm + q$ ). For the assumed positive potential applied to plane 1 the wavefunction amplitudes of these states are higher for layer 1 than for layer 2. Even though the induced magnetic moments are extremely small, the spin polarization at the Fermi level  $P_{BLG} = \frac{\varrho_\uparrow(E_F) - \varrho_\downarrow(E_F)}{\varrho_\uparrow(E_F) + \varrho_\downarrow(E_F)}$  might be strong if  $E_F$  is placed close to the upper edge. In the narrow energy range in this region the full spin polarization of electrons is observed. Apart from Van Hove singularities in the position of minima (maxima) of conduction band (valence band) also jumps of DOS are observed. They correspond to maximum (minimum) of energy in the centers of valleys (see the inset). Fig. 2 shows hybridization self energies for angular momentum symmetries  $m = 0, 1, 2$ . The presented hybridization function  $\Sigma_m$  plays the role of self-energy of the impurity Green's function  $G_0(\omega)$  corresponding to (3),  $\Sigma_m(\omega) = \omega - \epsilon_0 - G_0^{-1}(\omega)$ . As it is seen for hollow site hybridization of  $m = 0$  symmetry is strongly suppressed in the low energy range. The self-energies for  $m = 1$  and  $m = 2$  do not differ very much in this region, but for higher energies distinctive differences are observed and the dependences are strongly asymmetric with respect to the zero energy. Very roughly the electron part of  $m = 1$  self energy corresponds to the hole part of  $m = 2$ . The observed splitting of the peaks around  $E - E_F \approx 1.03$  corresponding to  $M$  point of Brillouin zone are caused by interlayer coupling. The details of the spin dependent structure around band gap are presented on Fig. 3, where in addition to imaginary parts also real parts of self energies are plotted. Divergence of imaginary part for  $E_F$  located at the edge signals non-Fermi liquid behavior. The observed peaks and jumps of the real part substantially renormalize

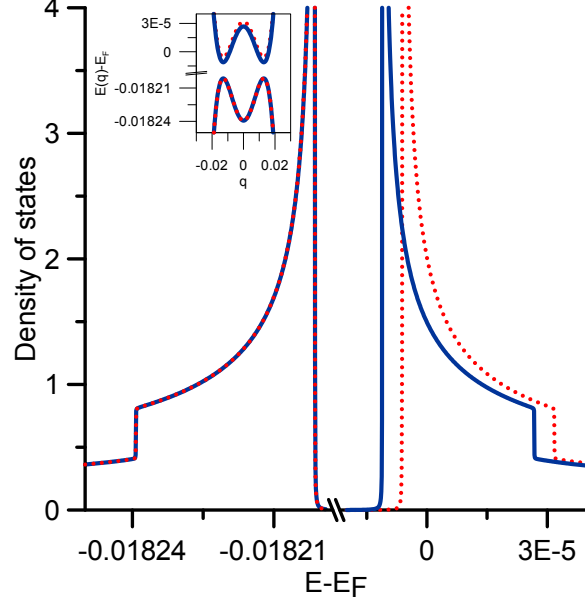


FIG. 1: (Color online) Spin-resolved densities of states of BLG close to the bandgap plotted by solid (dotted) line for up (down) spin. Inset shows the corresponding Hartree-Fock bands,  $V_g = 0.0185$ .

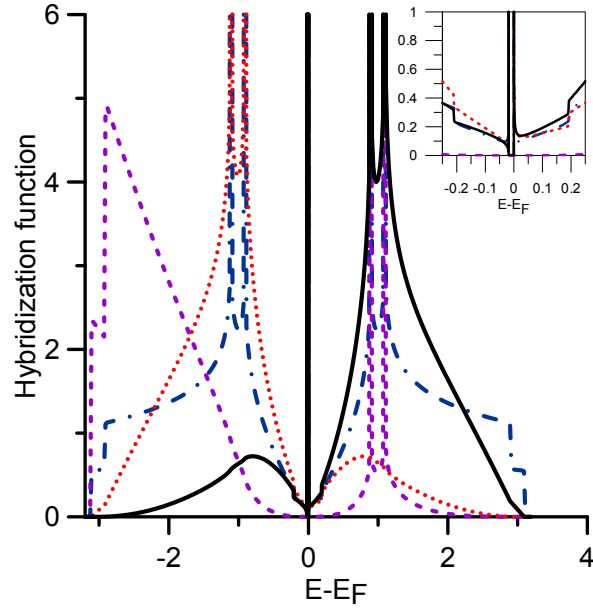


FIG. 2: (Color online) Rescaled imaginary parts of hybridization functions for the impurity in the hollow site for three angular momentum symmetries  $\Sigma_m/V^2$  ( $m = 0$  - dashed line,  $m = 1$  - dotted line,  $m = 2$  - solid line) compared with BLG density of states (dash dash dotted line). Inset shows the same hybridization functions as in the main picture, but in the narrower energy range. The assignment of the lines is preserved.

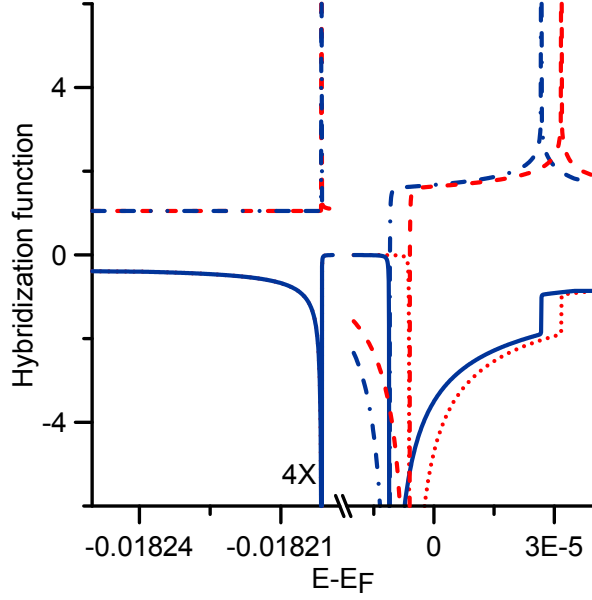


FIG. 3: (Color online) Real and imaginary parts of rescaled hybridization functions  $\Sigma_{1\sigma}/V^2$  plotted close to the bandgap. Solid and dotted lines represent imaginary parts for spin up and spin down respectively and dash dash dotted and dashed lines represent the real parts of the spin up and spin down self energies. For transparency imaginary part of hybridization function below the lower bandgap edge is extended four times.

the effective impurity energy level in this region. We do not address here the subtle problem of local moment formation in BLG, this has been recently discussed e.g. in [8]. We have only checked that in Hartree-Fock approximation the magnetic moment of impurities do not vanish for the assumed parameters. Figures 4 and 5 show evolution of the expectation values of slave boson operators, magnetic moment and polarization of impurity versus  $E_F$  for  $SU(2)$  and  $SU(4)$  symmetries. The factors determining the character of the many-body resonance are the deepness of the atomic level with respect to  $E_F$  and hybridization strength. For the narrow energy range discussed, where the dramatic changes of the latter are observed, impact of the hybridization is dominant. The representative densities of states of the impurity ( $\varrho_{0\sigma}(E)$ ) are shown on Figures 6. Below the lower gap edge, where hybridization self-energy is small, structureless and spin independent (Figs. 4a, 5a), typical Kondo resonance is formed centered at  $E_F$  for  $SU(2)$  symmetry and shifted above  $E_F$  for  $SU(4)$  case (Fig 6a). When  $E_F$  moves closer to the edge and both real and imaginary parts of self-energy are strongly enhanced broadening of many-body spectral function results for both symmetries

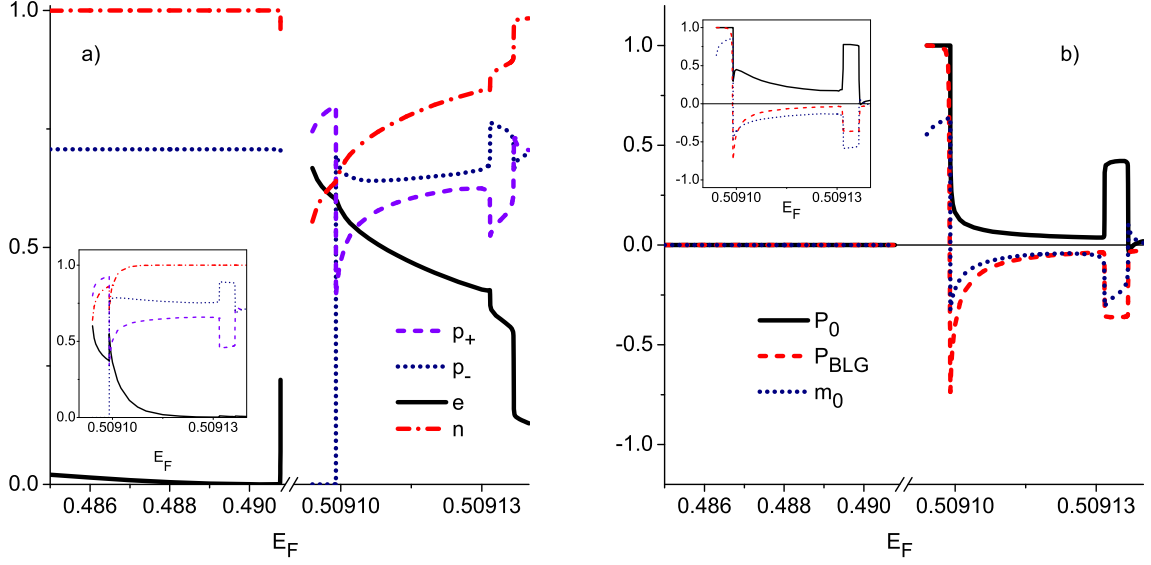


FIG. 4: (Color online) Evolution of  $SU(2)$  impurity state with the shift of the Fermi level in the narrow energy range around bandgap a) The expectation values of slave-boson operators  $e$ ,  $p_\sigma$  and the impurity electron occupation  $n$  for coupling parameter  $V = 0.25$ . b) Polarization of impurity  $P_0$ , impurity magnetization  $m_0$  and polarization of BLG ( $P_{BLG}$ ). Insets of both pictures present the corresponding dependences for  $V = 0.1$  for  $E_F$  located above the upper gap edge.

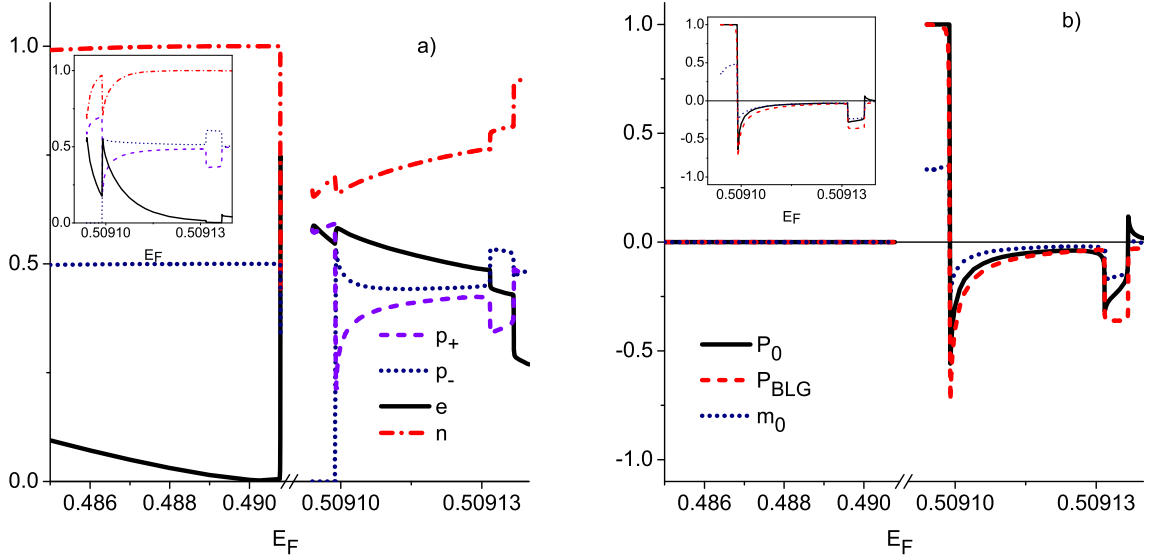


FIG. 5: (Color online) The same as in Fig. 4 but for  $SU(4)$  symmetry.

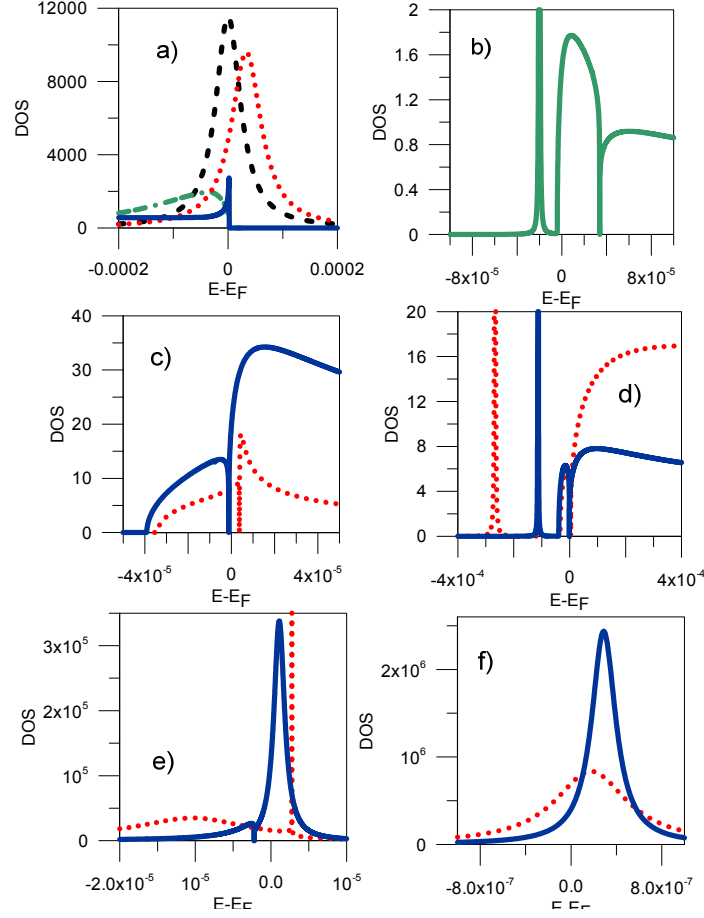


FIG. 6: (Color online) Representative impurity densities of states a)  $V = 0.25$ ,  $E_F$  located below lower bandgap edge (unpolarized BLG):  $SU(2)$   $E_F \approx 0.48580$  dashed line,  $SU(2)$   $E_F \approx 0.49080$  dash dash dotted line,  $SU(4)$   $E_F \approx 0.48580$  dotted line,  $SU(4)$   $E_F \approx 0.49080$  solid line, b)  $V = 0.25$ , DOS of orbital MV state  $SU(4) \rightarrow SU(2)$  for  $E_F \approx 0.50909$  (fully spin polarized BLG), c)  $V = 0.25$ ,  $SU(2)$ ,  $E_F$  located between the upper bandgap edge and nearby step in BLG DOS (polarized BLG) ( $E_F \approx 0.50913$ ), solid line for spin up, dotted line for spin down, d) the same as (c), but for  $SU(4)$  symmetry, e) the same as (c), but for  $V = 0.1$ , f) the same as (d), but for  $V = 0.1$ .

and for  $SU(4)$  additional structure at the edge is also visible reflecting a new pole in the impurity Green's function occurring close to the edge, but still in the region of finite density of states of BLG. Within the gap a resonance can be also formed, and in this case the resonance is not masked by finite DOS and takes the form of Dirac delta like line (Figs. 6b,d). Of interest are also dips in the impurity DOS (Figures 6b-e), occurring for energies



where steps in the imaginary parts and peaks in real parts of self energies are observed (Fig. 3). The narrow energy region above the upper edge is of special interest for spintronics, because spin polarization of BLG matrix results in spin splitting of resonances (Figs. 6c-f). For typical coupling parameter corresponding to the equilibrium distance of impurity from the graphene layer (assumed value  $V = 0.25$  corresponds to Co impurity-graphene coupling [6]), the calculated average occupation considerably deviates from  $n = 1$  i.e. impurity is in mixed valence state for both symmetries (Figs. 6c,d, Figs. 4a,5a). More interesting is the case of a weaker coupling, when the spin polarized Kondo state is formed (Figs. 6e,f). Possible reduction of the coupling can be achieved e.g. by chemical engineering (ligands), or introducing ultrathin dielectric film separating impurity from graphene layer, or putting the adatom further from the surface by STM methods [9]. For Fermi level located between the upper edge and nearest higher in energy step in BLG density of states the impurity polarization for  $SU(2)$  symmetry is opposite to BLG polarization, whereas for  $SU(4)$  has the same sign (Figs. 4b,5b). This tendency is observed both in MV and in Kondo states and is in agreement with earlier calculations for regular density of states of the electrodes performed with the use of different techniques [10–12]. This behavior reflects the fact that despite the same sign of the spin splitting for both symmetries (opposite to BLG spin splitting), the dominance of spin resolved densities of states at the Fermi level is different due to significantly different location of unperturbed many-body peaks in  $SU(2)$  and  $SU(4)$  cases. Interesting observation is a possibility of full spin-polarization of impurity state in the region of full polarization of BLG matrix and reverse of magnetic moment when  $E_F$  enters the region of full BLG spin polarization. Since the Fermi level can be shifted by gate voltage this gives the way of electric control of magnetic moment, what is a highly desirable property for spintronics.

In summary, present investigation only signals the interplay of different factors on the many-body physics of magnetic impurity in bilayer graphene doped near the Van Hove singularity at the bandgap edges. The exact description of the crossing of the Fermi energy with a Van Hove singularity in the DOS would require more sophisticated methods, both in defining the magnetic state of the bilayer going beyond mean field scheme and in discussion of screening processes, where analysis outside SBMFA is required. In addition to hole-like processes discussed above also electron-like charge fluctuations might play the role in reconstruction of Kondo resonance and this topic will be the subject of a forthcoming paper.

## Acknowledgments

This work was supported by the Polish Ministry of Science and Higher Education as a research project No. N N202199239 in years 2010 – 2013.

---

- [1] S. Das Sarma, S. Adam, E.H. Hwang, and E. Rossi, *Rev. Mod. Physics* **83**, 407 (2011).
- [2] Y. Zhang, T.-T. Tang, C. Girit, Z. Hao, M. C. Martin, A. Zettl, M. F. Crommie, Y. R. Shen and F. Wang, *Nature* **459**, 820 (2009).
- [3] J. Nilsson, A. H. Castro Neto, N. M. R. Peres, and F. Guinea, *Phys. Rev. B* **73**, 214418 (2006).
- [4] T. Stauber, N. M. R. Peres, F. Guinea, and A. H. Castro Neto, *Phys. Rev. B* **75**, 115425 (2007).
- [5] E. V. Castro, N. M. R. Peres, T. Stauber, and N. A. P. Silva, *Phys. Rev. Lett.* **100**, 186803 (2008).
- [6] T. O. Wehling, A. V. Balatsky, M. I. Katsnelson, A. I. Lichtenstein, and A. Rosch, *Phys. Rev. B* **81**, 115247 (2010).
- [7] G. Kotliar and A. E. Ruckenstein, *Phys. Rev. Lett.* **57**, 1362 (1986).
- [8] M. Killi, D. Heidarian, and A. Paramekanti, *New J. Phys.* **13**, 053043 (2011).
- [9] M. Ternes, A. J. Heinrich, and W. D. Schneider, *J. Phys.: Condens. Matter* **21**, 053001 (2009).
- [10] J. Martinek, Y. Utsumi, H. Imamura, J. Barnaś, S. Maekawa, J. König, and G. Schön, *Phys. Rev. Lett.* **91**, 247202 (2003).
- [11] M. S. Choi, D. Sanchez, and R. López, *Phys. Rev. Lett* **92**, 056601 (2004).
- [12] S. Lipiński and D. Krychowski, *Phys. Rev. B* **81**, 115327 (2011).